Bull. Chem. Soc. Ethiop. **2026**, 40(12), 2535-2545.
DOI: https://dx.doi.org/10.4314/bcse.v40i12.3
© 2026 Chemical Society of Ethiopia and The Authors
ISSN 1011-3924
Printed in Ethiopia
Online ISSN 1726-801X

HETEROMETALLIC COORDINATION COMPOUNDS OF LEAD(II) ACETATE WITH COBALT(II), NICKEL(II), AND COPPER(II) FORMATES: SYNTHESIS, STRUCTURE, AND PROPERTIES

Zubayda Shavkatovna Abdullaeva[1,2], Shakhnoza Abdukhalilovna Kadirova[3], Shodlik Bekpulatovich Khasanov[1], Mavlyuda Matyakubova[4], Farhod Karimovich Khallokov[5], Abdullo Amrullojon Oglu Ahadov[5,6,*], Olim Bobomurodovich Rakhmatov[7]

[1]Khorezm Academy of Mamun, Khiva 220900, Uzbekistan
[2]Urgench Ranch University of Technology, Urgench 220100, Uzbekistan
[3]Department of Inorganic Chemistry, National University of Uzbekistan, Tashkent 100174, Uzbekistan
[4]Department of Food Technology, Urganch State University, Urgench 220100, Uzbekistan
[5]Department of Biomedical Engineering, Biophysics, and Informatics, Bukhara State Medical Institute, Bukhara 200100, Uzbekistan
[6]Department of Physics, Bukhara State University, Bukhara 200100, Uzbekistan
[7]Department of Dermatovenerology and Pediatric Dermatovenerology, Bukhara State Medical Institute, Bukhara 200100, Uzbekistan

(Received September 25, 2025; Revised April 13, 2026; Accepted August 17, 2026)

ABSTRACT. We established optimal synthesis conditions for heterometallic coordination compounds of lead(II) acetate with cobalt(II), nickel(II), and copper(II) formates. The synthesized complexes were characterized by elemental analysis using energy-dispersive spectroscopy (EDS), confirming the consistency between experimental and calculated data. During the research, we developed optimal conditions for synthesizing the complex compounds and obtained new coordination compounds in high yield. The composition of the synthesized compounds was studied using scanning electron microscopy and energy-dispersive X-ray analysis (SEM-EDX), and the experimental elemental quantities were found to be in reasonable agreement with the theoretically calculated values. Based on the elemental analysis, we proposed the empirical formulas of the new complexes. The results of IR spectroscopy confirmed the formation of heterometallic complexes through the bidentate-bridging coordination of acetate anions. Data from diffuse reflectance electronic spectroscopy indicated that the metal ions have a coordination number of 6 and an octahedral coordination environment. Quantum-chemical calculations (DFT, B3LYP/3-21G) were performed to determine the optimized molecular geometries, bond lengths, charge distributions, HOMO–LUMO energies, and ionization potentials. Thermal analysis revealed decomposition, melting, and sublimation processes, with a total mass loss of 60-80% and the formation of metal oxides. Molar conductivity results showed that the complex compounds are neutral, confirming their structural model.

KEY WORDS: Cobalt(II) formate, Nickel(II) formate, Copper(II) formate, Lead(II) acetate, IR spectroscopy, Elemental analysis, Thermal analysis, Diffuse reflectance electronic spectra

INTRODUCTION

The synthesis of new binuclear mixed-ligand coordination compounds and the investigation of their structural [1-3] and physicochemical properties have attracted considerable attention worldwide due to their promising functional characteristics and broad application potential in modern science and technology [4-6]. Among such compounds, systems exhibiting luminescent [7-9], stimulatory [10-13], and magnetic properties [14-16] are of particular interest, since they open new opportunities for practical use in diverse areas of the economy and advanced materials research.

*Corresponding author. E-mail: ahadov.abdullo@bsmi.uz
This work is licensed under the Creative Commons Attribution 4.0 International License

In addition to their multifunctionality, coordination compounds of this class are distinguished by their ability to form clusters owing to the presence of multiple metal centers [17,18]. Such polynuclear heterometallic complexes have been successfully applied as carriers of biologically active substances in living organisms, as well as in catalysis and materials engineering [19, 20].

Recent studies have therefore focused on optimizing the synthesis conditions of polynuclear heterometallic coordination compounds [21, 22], as well as on designing bioactive agents, growth stimulants [23, 24], and highly effective insecticides with multifunctional action. Within this context, an important research direction involves the rational development of formate–acetate metal complexes with transition metal ions, along with a detailed determination of their composition, structure, and physicochemical properties.

The primary objective of this research is to synthesize new heterometallic coordination compounds of cobalt(II), nickel(II), and copper(II) formates with lead(II) acetate, and to study their structures and physicochemical properties.

EXPERIMENTAL

Synthesis of coordination compounds of Co(II), Ni(II), and Cu(II) formates with Pb(II) acetate: A mixture of 0.01 mol of metal formate ($Co(HCOO)_2$ 1.47 g, $Ni(HCOO)_2$ 1.47 g, $Cu(HCOO)_2$ 1.52 g) and 0.02 mol (13 g) of lead(II) acetate was prepared in glacial acetic acid (Figure 1). The reaction mixture was refluxed for 1.5 hours, then filtered and concentrated on a rotary evaporator to a dry residue. The resulting residue was dissolved in 20 mL of acetonitrile, evaporated to 10 mL, and left to stand for 24 hours.

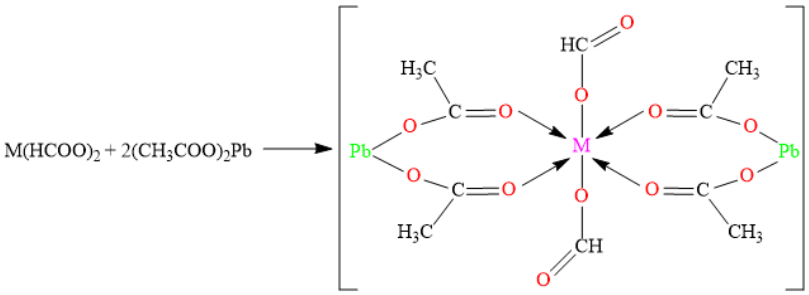

Figure 1. Proposed reaction scheme for the synthesis of heterometallic coordination complexes $[M(HCOO)_2 \cdot 2Pb(CH_3COO)_2]$ (M = Co(II), Ni(II), Cu(II)) from metal formates and lead(II) acetate.

Table 1. Elemental analysis and physical properties of complex compounds.

Compounds		$[Co(HCOO)_2 \cdot 2Pb(CH_3COO)_2]$	$[Ni(HCOO)_2 \cdot 2Pb(CH_3COO)_2]$	$[Cu(HCOO)_2 \cdot 2Pb(CH_3COO)_2]$
M	Calculated	7.371	7.343	7.902
	Found	7.1	7.2	7.9
Pb	Calculated	51.830	51.845	51.532
	Found	50.3	50.3	51.4
C	Calculated	15.022	15.027	14.936
	Found	17.5	17.5	14.7
O	Calculated	24.012	24.019	23.874
	Found	23.3	23.3	24.3
Color		Light pink	White	Light green
Melting point, °C		133	200	97
Yield, %		81	67	64

Solvent solubility	Water	Sparingly soluble	Sparingly soluble	Sparingly soluble
	Ethanol	Soluble	Soluble	Soluble
	Acetonitrile	Insoluble	Sparingly soluble	Sparingly soluble
	Benzene	Insoluble	Insoluble	Insoluble
	Acetone	Insoluble	Sparingly soluble	Insoluble
	DMF	Insoluble	Insoluble	Insoluble

RESULTS AND DISCUSSION

The elemental analysis and microstructure of the synthesized compounds were determined using an SEM EVO MA 10 (Zeiss) scanning electron microscope equipped with an Aztec Energy Advanced X-Act (Oxford Instruments) energy-dispersive X-ray spectrometer (Figures 2-4).

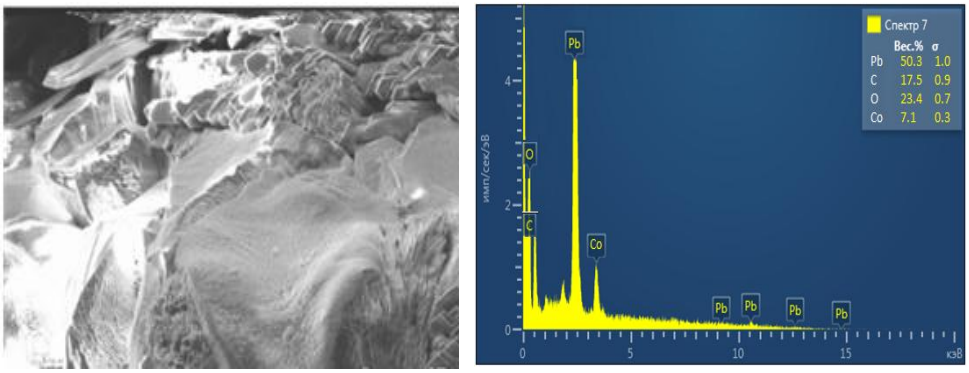

Figure 2. Microstructure and EDS results of $[Co(HCOO)_2 \cdot 2Pb(CH_3COO)_2]$.

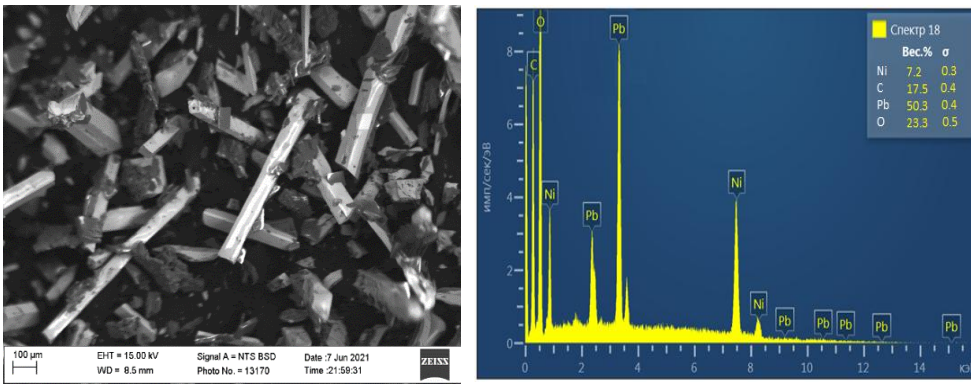

Figure 3. Microstructure and EDS results of $[Ni(HCOO)_2 \cdot 2Pb(CH_3COO)_2]$.

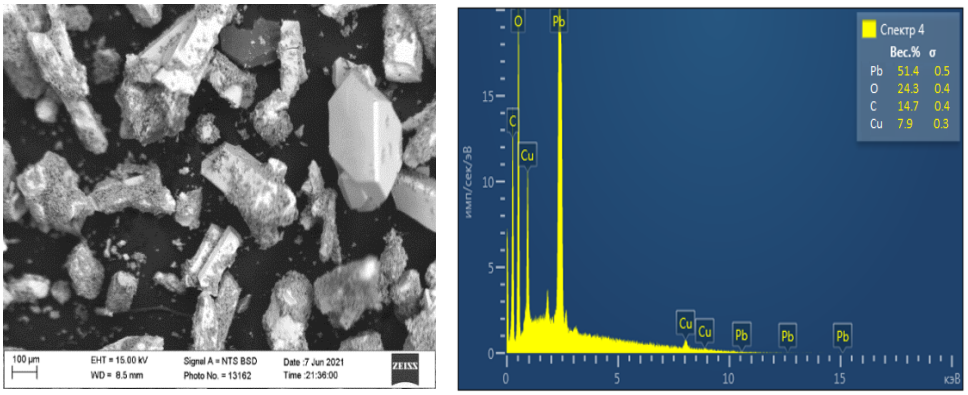

Figure 4. Microstructure and EDS results of $[Cu(HCOO)_2 \cdot 2Pb(CH_3COO)_2]$.

The surface morphology of the synthesized complexes, namely $[Co(HCOO)_2 \cdot 2Pb(CH_3COO)_2]$, $[Ni(HCOO)_2 \cdot 2Pb(CH_3COO)_2]$, and $[Cu(HCOO)_2 \cdot 2Pb(CH_3COO)_2]$, was investigated using scanning electron microscopy (SEM).

The SEM image of the Co-based complex reveals a relatively homogeneous microstructure composed of fine, granular particles. The particles are moderately agglomerated, forming a compact but slightly irregular surface. This suggests a stable nucleation process with controlled crystal growth [25].

In contrast, the Ni-based complex exhibits a denser and more compact morphology with well-defined grain boundaries. The particles appear larger and more crystalline compared to the Co analogue. The higher degree of agglomeration and structural uniformity indicates enhanced crystallization, which can be attributed to the stronger crystal field stabilization and smaller ionic radius of Ni^{2+} ions.

The Cu-based complex demonstrates a significantly different morphology. The structure is irregular, with plate-like and elongated (anisotropic) features, along with noticeable porosity. This non-uniform growth behavior is likely associated with the Jahn–Teller distortion characteristic of Cu^{2+} ions, which induces lattice asymmetry and disrupts uniform crystal formation.

EDS analysis was performed to determine the elemental composition of the synthesized complexes. The spectra confirm the presence of Pb, O, and C in all samples, along with the corresponding transition metal ions (Co, Ni, and Cu), consistent with the proposed chemical formulas. For the Co-based complex, the elemental distribution is relatively uniform, with moderate intensity peaks corresponding to Co, Pb, O, and C. This indicates successful incorporation of all components within the structure. The Ni-based complex shows a more homogeneous elemental distribution with relatively stronger and sharper metal peaks. This suggests improved compositional uniformity and supports the SEM observation of a well-developed crystalline structure. In the case of the Cu-based complex, the EDS spectra reveal slight variations in elemental distribution, with localized intensity fluctuations. This heterogeneity correlates well with the observed irregular and porous morphology in SEM images, further confirming the structural distortion effects associated with Cu^{2+} ions.

A comparative evaluation of the three complexes indicates that the nature of the transition metal ion plays a crucial role in determining both microstructure and compositional uniformity.

Among the studied systems, the Ni-based complex exhibits the highest degree of structural order, crystallinity, and elemental homogeneity. The Co-based complex shows intermediate characteristics, maintaining relatively uniform morphology with moderate crystallinity. In contrast, the Cu-based complex displays the lowest structural order, characterized by anisotropic growth, higher porosity, and less uniform elemental distribution.

These differences can be explained by the electronic configurations of the metal ions. In particular, the Jahn–Teller effect in Cu^{2+} leads to lattice distortion, whereas Ni^{2+} promotes stable and symmetric crystal formation.

Overall, the combined SEM and EDS results demonstrate that all synthesized complexes were successfully formed with the intended composition. However, their structural properties vary significantly depending on the central metal ion. The Ni-based complex shows superior crystallinity and homogeneity, while the Cu-based complex exhibits structural distortion and heterogeneity. The Co-based complex lies between these two extremes.

The synthesized complexes were investigated using IR spectroscopic analysis. The diffuse reflectance spectra of the obtained compounds were also analyzed, and their thermal stability was determined. Additionally, the energies and geometrical parameters of the molecules were determined through quantum-chemical calculations. Based on these results, the structures of the synthesized complexes were proposed [26].

The results of measurements of molar electrical conductivity showed that all the synthesized complexes have properties similar to non-electrolytes, which confirms their neutral nature and non-dissociation into ions in solution. This indicates that the ligands are coordinated in the inner sphere of the metal ions. In addition, the calculated stability constants demonstrate sufficient stability of the complexes and support the proposed structures. Thus, data on electrical conductivity and stability confirm the formation of neutral coordination compounds [27].

To determine the spatial structure and the coordination number of the central metal atom in the coordination compounds, the input file was generated by the non-empirical method using the *HyperChem 8.07* program within the MINIMAL STO-3G approximation and further optimized by the *Gaussian 09* program at the 3-21G B3LYP level of theory [28]. The optimal spatial structures of the molecules, the distribution of atomic charges, as well as the bond orders and bond lengths, were determined. The energies of the highest occupied and lowest unoccupied molecular orbitals (HOMO and LUMO) were calculated, and the ionization potential was obtained.

Based on quantum-chemical calculations, the most favorable geometries of the coordination node were determined, along with the bond lengths and atomic charge distributions. The calculated heats of formation, as well as the energies of the highest occupied (HOMO) and lowest unoccupied (LUMO) molecular orbitals, are presented in Table 2.

Table 2. Optimized parameters of synthesized compounds.

№	Compound	Heat of formation (kcal·mol^{-1})	HOMO (eV)	LUMO (eV)	Δ (LUMO–HOMO, eV)
1	$[Cu(HCOO)_2{\cdot}2Pb(CH_3COO)_2]$	-527.18	-9.63	-0.57	9.06
2	$[Ni(HCOO)_2{\cdot}2Pb(CH_3COO)_2]$	-411.36	-7.47	-1.29	6.18
3	$[Co(HCOO)_2{\cdot}2Pb(CH_3COO)_2]$	-378.73	-7.68	-0.83	6.85

The parameter Δ (LUMO–HOMO) represents the excitation potential of the molecule. The smaller the Δ value, the more easily the molecule undergoes excitation and exhibits higher reactivity. Therefore, the $[Ni(HCOO)_2{\cdot}2Pb(CH_3COO)_2]$ complex is considered the most reactive among the synthesized compounds.

Analysis of coordination compounds of transition-metal formates with lead(II) acetate revealed noticeable changes in the IR spectra. The most pronounced modifications were observed in the M–O bond region, as well as in the asymmetric and symmetric stretching vibrations of the acetate group [29]. This behavior indicates that the acetate anion, initially coordinated in a monodentate fashion, transforms into a bidentate-bridging coordination mode upon complex formation. In the initial metal acetates, the M–O stretching vibrations were observed at 461-476 cm^{-1} and 503-567 cm^{-1}. After coordination, these bands shifted to 426-500 cm^{-1} and 503-615 cm^{-1}. In addition, the characteristic absorption bands of the Me–O vibrations in free acetates

at 615-638 cm^{-1} and 648-689 cm^{-1} were shifted to 608-654 cm^{-1} and 652-700 cm^{-1} in the synthesized complexes.

In the spectra of the initial metal acetates, the symmetric and asymmetric stretching vibrations of the acetate anion were observed at $\nu_s(COO^-)$ = 1380-1447 cm^{-1} and $\nu_{as}(COO^-)$ = 1531-1551 cm^{-1}, respectively [29]. Upon coordination, these absorption bands shifted to $\nu_s(COO^-)$ = 1371-1443 $cm^{-1}$and $\nu_{as}(COO^-)$ = 1514-1609 cm^{-1}. This shift is consistent with bidentate-bridging coordination, indicating that the acetate anion coordinates to the central transition-metal atom through a bridging mode. Additional evidence for acetate groups in the synthesized complexes comes from the deformation and stretching vibrations of the methyl groups, observed in the IR spectra at 1013-1036 cm^{-1} and 2797-2988 cm^{-1}.

The characteristic vibrational frequencies of the synthesized complexes were determined as follows: for the $[Cu(HCOO)_2 \cdot 2Pb(CH_3COO)_2]$ complex, the δ(M–O) vibration was observed at 654 cm^{-1}, while the symmetric stretching vibration $\nu_s(COO^-)$ appeared at 1373 cm^{-1} and the asymmetric stretching vibration $\nu_{as}(COO^-)$ at 1520 cm^{-1}.

For the $[Co(HCOO)_2 \cdot 2Pb(CH_3COO)_2]$ complex, the δ(M–O) vibration was recorded at 615 cm^{-1}, with $\nu_s(COO^-)$ at 1394 cm^{-1} and $\nu_{as}(COO^-)$ at 1557 cm^{-1}.

In the case of the $[Ni(HCOO)_2 \cdot 2Pb(CH_3COO)_2]$ complex, the δ(M–O) vibration was observed at 700 cm^{-1}, while the $\nu_s(COO^-)$ and $\nu_{as}(COO^-)$ vibrations appeared at 1417 cm^{-1} and 1593 cm^{-1}, respectively.

These results confirm the coordination of formate and acetate groups with metal ions and support the structural features of the synthesized complexes.

Thus, IR spectroscopic analysis confirmed that the synthesized compounds are polynuclear heterometallic coordination complexes formed via bidentate-bridging coordination of acetate groups [30]. To determine the geometry and coordination number of the hexacoordinated central metal atoms, diffuse reflectance electronic spectra were recorded and analyzed. In octahedral high-spin cobalt(II) complexes, three characteristic transitions are typically observed: $^4T_{1g}(F) \rightarrow {}^4T_{2g}$, $^4T_{1g}(F) \rightarrow {}^4A_{2g}$, and $^4T_{1g}(F) \rightarrow {}^4T_{1g}(P)$, which appear in the region around 20000 cm^{-1}. Additional transitions are observed at 8500–10000 cm^{-1}, also characteristic of hexacoordinated cobalt(II) complexes. In the synthesized cobalt(II) complexes, diffuse reflectance spectra displayed bands at 9653, 17123, and 19608 cm^{-1}, confirming the octahedral geometry of the coordination environment (Figure 5).

In octahedral nickel(II) complexes, reflection spectra are generally observed in the regions 8000-13000, 13000-17000, and 19000-27000 cm^{-1}. For the synthesized Ni(II) complexes, the diffuse reflectance spectra revealed bands at 10060, 14727, and 22421 cm^{-1}, as well as at 8445, 12836, and 21978 cm^{-1}.

For the copper(II) complexes, diffuse reflectance spectra exhibited bands at 9500 and 14000 cm^{-1}. The shift of the transition region within such a narrow range can be explained by the triply degenerate Cu(II) ion and the Jahn–Teller effect. According to crystal field theory, this effect arises from the splitting of electronic levels, leading to excess energy that distorts the octahedral configuration through elongation or compression. As a result, the octahedral geometry of the copper(II) complexes deviates from the ideal structure.

The analysis of diffuse reflectance spectra of the synthesized complexes revealed characteristic absorption bands at 9990, 13661 cm^{-1} and 9920, 14598 cm^{-1}, confirming the octahedral environment of the central metal atoms.

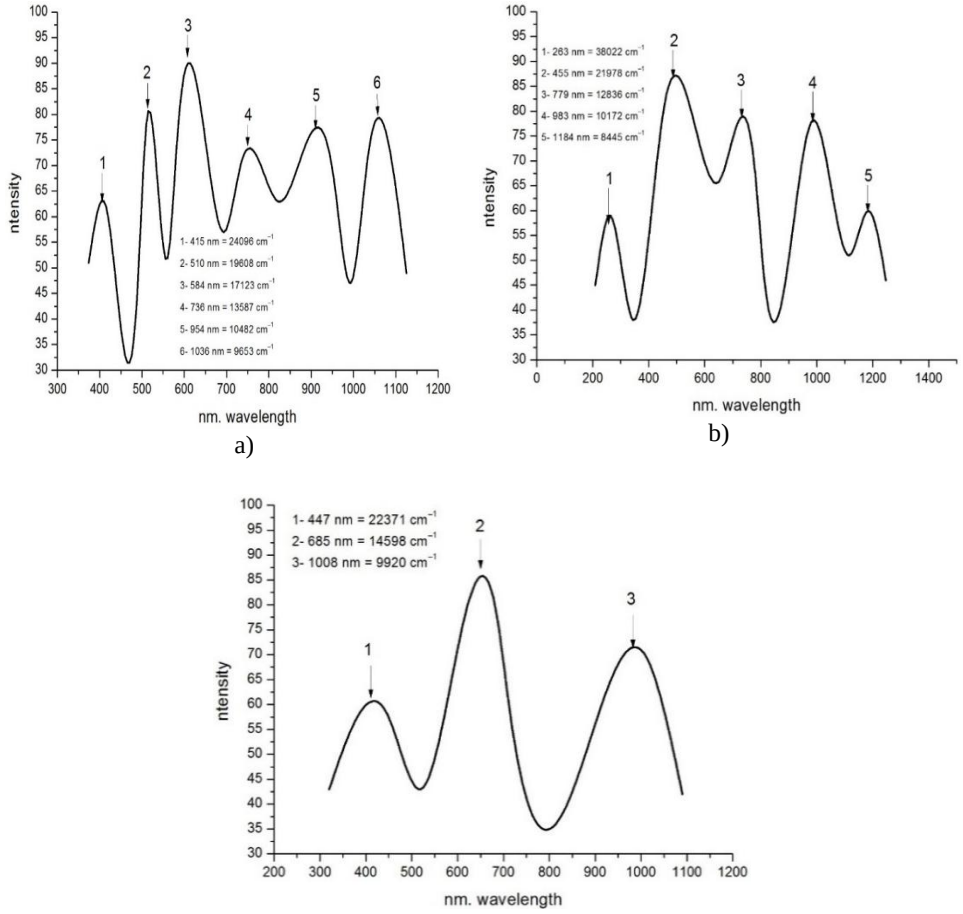

Figure 5. DRES of $[Co(HCOO)_2 \cdot 2Pb(CH_3COO)_2]$ (a), $[Ni(HCOO)_2 \cdot 2Pb(CH_3COO)_2]$ (b) and $[Cu(HCOO)_2 \cdot 2Pb(CH_3COO)_2]$ (c) complexes.

The stability constants of the complexes formed in aqueous solutions by the interaction of Co(II), Ni(II), and Cu(II) formates with lead(II) acetate were determined using the photometric method (Table 3). Absorption spectra of the studied systems were obtained, and the maximum absorption wavelengths were identified. The stability constants of the complexes were calculated by the Babko dilution method.

The experimental data show that the values of the stability constants of the complexes formed in aqueous solution, calculated by the Babko dilution method, are satisfactory at a metal formate to lead(II) acetate ratio of 1:2. According to the results, the stability of the coordination compounds increases in the order Co(II) < Ni(II) < Cu(II). The nature and coordination number of the ligand do not exhibit a significant influence in this case.

Table 3. Results of determination of the stability constant of Co(II), Ni(II), and Cu(II) formate acetate complexes by the Babko dilution method.

№	Complex	$C_1 \cdot 10^{-5}$, (mol/L)	A_1	$C_2 \cdot 10^{-5}$, (mol/L)	A_2	$K_{(ML^n)}$ (β_k)	$lgK_{(ML^n)}$ ($lg\beta_k$)
1	$[Cu(HCOO)_2 \cdot 2Pb(CH_3COO)_2]$	7.92	0.148	4.58	0.076	5.48×10^6	6.74
2	$[Ni(HCOO)_2 \cdot 2Pb(CH_3COO)_2]$	1.16	0.220	4.47	0.112	5.19×10^5	5.715
3	$[Co(HCOO)_2 \cdot 2Pb(CH_3COO)_2]$	9.60	0.122	3.27	0.052	1.5×10^5	5.18

In order to determine the thermal properties of the synthesized complexes, thermal analysis was carried out using a Paulik–Paulik–Erdey derivatograph at a heating rate of 10 °C/min with a sample mass of 0.1 g (Figure 6). The study revealed the presence of various phase transitions in the coordination compounds within the temperature range of 140-200 °C, which indicates that the observed endothermic effects occur without a change in mass. Exothermic effects observed above 200 °C correspond to the breaking of coordination bonds, decomposition of formates and acetates, and combustion of thermolysis products. The total mass loss during thermal decomposition amounts to 60-66%, with the corresponding metal oxides (CoO, NiO, CuO, and PbO) formed as the final products.

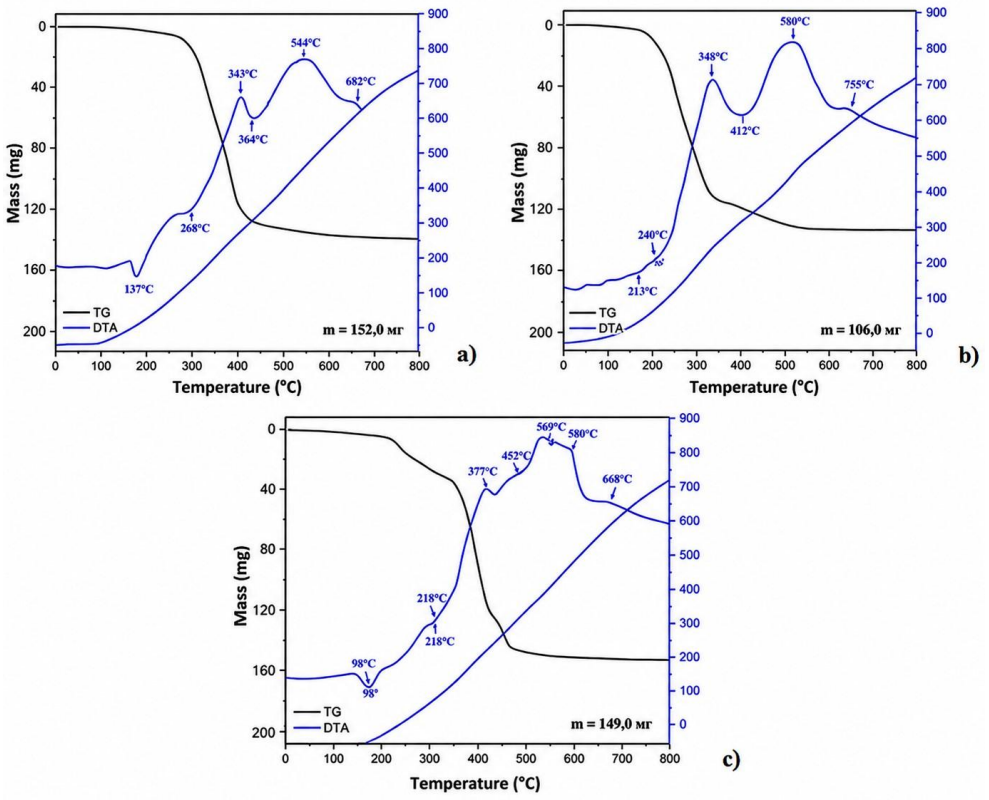

Figure 6. Derivatograms of the compounds $[Co(HCOO)_2 \cdot 2Pb(CH_3COO)_2]$ (a), $[Ni(HCOO)_2 \cdot 2Pb(CH_3COO)_2]$ (b) and $[Cu(HCOO)_2 \cdot 2Pb(CH_3COO)_2]$ (c).

CONCLUSION

In this study, novel heterometallic complexes of Co(II), Ni(II), and Cu(II) formates with Pb(II) acetate were synthesized, and their structures and properties were investigated using a range of methods. The research results revealed the bidentate-bridging coordination of the acetate ligands and the octahedral geometry of the complexes. Molar conductivity data confirmed their neutral and non-electrolytic nature. The stability and structural features indicate a high degree of organization within the complexes. Trinuclear complexes of Co(II), Ni(II), and Cu(II) formates with lead(II) acetate were synthesized, and their composition, structure, and properties were determined using elemental analysis, differential thermal analysis, IR spectroscopy, electronic spectroscopy, and scanning electron microscopy. The results confirmed the formation of octahedral coordination compounds. The spatial structures, as well as the energetic and geometrical parameters of the synthesized complexes, were analyzed using the Gaussian 09 software package, with GaussView employed for building and visualizing model systems at the B3LYP level within the framework of DFT. The stability constants of the reactions leading to the formation of formate–acetate coordination compounds of transition metals were calculated, and it was shown that the stability increases in the order Co(II) < Ni(II) < Cu(II), in agreement with the Irving–Williams series for divalent metal ions. The thermal stability of the synthesized compounds was determined by differential thermal analysis (DTA), and it was found that the thermal stability of the complexes increases in the sequence Co(II) < Ni(II) < Cu(II). These findings provide an important scientific basis for the synthesis of heterometallic coordination compounds and their practical applications, particularly in catalysis and the development of new functional materials.

Credit authorship contribution statement

Z.Sh. Abdullaeva: Writing – review and editing, Writing – original draft, Visualization, Validation, Software, Resources, Project administration, Methodology, Investigation, Formal analysis, Data curation, Conceptualization.
Sh.A. Kadirova: Writing – review and editing, Writing – original draft, Visualization, Validation, Software, Resources, Methodology, Investigation, Formal analysis, Data curation, Conceptualization.
Sh.B. Khasanov: Writing – review and editing, Writing – original draft, Visualization, Validation, Software, Resources, Methodology, Investigation, Formal analysis, Data curation, Conceptualization.
M. Matyakubova: Writing – review and editing, Writing – original draft, Visualization, Validation, Software, Resources, Methodology, Investigation, Formal analysis, Data curation, Conceptualization.
F.K. Khallokov: Writing – review and editing, Validation, Software, Resources, Project administration, Formal analysis, Conceptualization
A. Ahadov: Writing – review and editing, Validation, Software, Resources, Project administration, Investigation, Formal analysis, Conceptualization.
O.B. Rakhmatov: Resources, Project administration, Methodology, Investigation, Formal analysis, Conceptualization.

Data availability: The original contributions presented in the study are included in the article; further inquiries can be directed to the corresponding author.

Competing interests: The authors declare no competing interests.

Funding declaration: There is no funding for this work.

REFERENCES

1. Ismail, B.A.; Abd El-Wahab, Z.H.; Ali, O.A.M.; Nassar, D.A. Synthesis, structural characterization, and antimicrobial evaluation of new mononuclear mixed ligand complexes based on furfural-type imine ligand, and 2,2′-bipyridine. *Sci. Rep.* **2023**, 13, 9196.
2. Deka, B.; Sarkar, T.; Bhattacharyya, A.; Butcher, R.J.; Banerjee, S.; Deka, S.; Saikia, K.K.; Hussain, A. Synthesis, characterization, and cancer cell-selective cytotoxicity of mixed-ligand cobalt(III) complexes of 8-hydroxyquinolines and phenanthroline bases. *Dalton Trans.* **2024**, 53, 4952-4961.
3. Sathvara, J.P.; Jadeja, R.N.; Butcher, R.J. Synthesis, characterization, and crystal features of a mixed-ligand binuclear zinc(II) acyl-pyrazolone complex: DFT, Hirshfeld surface analysis and anti-malarial activity evaluation. *Inorg. Chim. Acta* **2024**, 573, 122316.
4. Alhazmi, F.S.; Morad, M.; Abou-Melha, K.; El-Metwaly, N.M.; Gashaw, W. Synthesis and characterization of new mixed-ligand complexes; density functional theory, Hirshfeld, and in silico assays strengthen the bioactivity performed in vitro. *ACS Omega* **2023**, 8, 4220-4233.
5. Yu, A.; Jiang, W.; Shen, Y.; Zhang, Y. Binuclear Pt(II) complexes with N∧C∧N ligands: synthesis, photophysical properties, and vapochromic responses. *Cryst. Growth Des.* **2025**, 25, 1872-1879.
6. Singh, A.; Boro, B.; Maji, A.; Butcher, R.J.; Banerjee, S. Design and synthesis of dinuclear cobalt(II) complexes derived from strong π-acidic ligands: crystal structure and studies on the oxidation of sp^3 C–H bonds. *New J. Chem.* **2023**, 47, 8951-8960.
7. Guo, X.Q.; Zhou, L.P.; Hu, S.J.; Sun, Q.F. Subtle adjustments for constructing multi-nuclear luminescent lanthanide organic polyhedra with triazole-based chelates. *Dalton Trans.* **2024**, 53, 4772-4780.
8. Hasegawa, Y.; Kitagawa, Y.; Nakanishi, T. Effective photosensitized, electrosensitized, and mechanosensitized luminescence of lanthanide complexes. *NPG Asia Mater.* **2018**, 10, 52-70.
9. Hasegawa, Y. Photofunctional lanthanoid complexes, coordination polymers, and nanocrystals for future photonic applications. *Bull. Chem. Soc. Jpn.* **2014**, 87, 1029-1057.
10. Sarkar, M. Binuclear transition metal complexes containing metal–metal bonds: Understanding the fundamental aspects and metal–metal cooperativity in catalysis. *Inorg. Chim. Acta* **2024**, 572, 122275.
11. Juyal, V.K.; Thakuri, S.C.; Panwar, M.; Prakash, O.; Nand, V.; Sharma, R. Manganese(II) and zinc(II) complexes of bidentate Schiff base ligands: Synthesis, structural characterization, antioxidant, antibacterial, and molecular docking studies. *Front. Chem.* **2024**, 12, 1414646.
12. Kaur, M.; Kapila, A.; Yempally, V.; Kaur, H. Synthesis, structural elucidation, and catalytic activity of bimetallic rhenium–tin complexes containing Schiff base ligand. *J. Mol. Struct.* **2022**, 1249, 131545.
13. Deka, B.; Sarkar, T.; Bhattacharyya, A.; Butcher, R.J.; Banerjee, S.; Hussain, A. Synthesis, characterization, and magnetic properties of mixed-ligand cobalt(III) complexes of 8-hydroxyquinolines and phenanthroline bases. *Dalton Trans.* **2024**, 53, 4952-4961.
14. Travadi, M.; Jadeja, R.N.; Butcher, R.J.; Banerjee, S. Magnetic behavior and crystal features of pentagonal uranyl acylpyrazolone complexes along with DFT calculation. *ACS Omega* **2022**, 7, 34359-34369.
15. Roccanova, R.; Ming, W.; Whiteside, V.R.; McGuire, M.A.; Sellers, I.R.; Du, M.-H.; Saparov, B. Synthesis, crystal and electronic structures, and optical properties of $(CH_3NH_3)_2CdX_4$ (X = Cl, Br, I). *Inorg. Chem.* **2017**, 56, 13878-13888.
16. Liddle, S.T.; van Slageren, J. Improving f-element single-molecule magnets. *Chem. Soc. Rev.* **2015**, 44, 6655-6669.
17. Craig, G.A.; Murrie, M. 3d single-ion magnets. *Chem. Soc. Rev.* **2015**, 44, 2135-2147.
18. Pinkowicz, D.; Podgajny, R.; Nowicka, B.; Chorazy, S.; Lis, T. Magnetic clusters based on octacyanidometallates. *Inorg. Chem. Front.* **2015**, 2, 10-27.

19. Wilson, R.J.; Lichtenberger, N.; Weinert, B.; Dehnen, S. Intermetalloid and heterometallic clusters combining p-block (semi)metals with d- or f-block metals. *Chem. Rev.* **2019**, 119, 8506-8554.
20. Chipman, J.A.; Berry, J.F. Paramagnetic metal–metal bonded heterometallic complexes. *Chem. Rev.* **2020**, 120, 2409-2447.
21. Ibragimov, B.T.; Khasanov, Sh.B.; Khudoyberganov, O.I.; Abdullaeva, Z.Sh.; Eshchanov, E.U. Synthesis and analysis of coordination compounds of nickel(II) acetate with monoethanolamine and p-nitrobenzoic acid. *Azerb. Chem. J.* **2022**, 4, 43-47.
22. Khasanov, Sh.B.; Ibodullaeva, T.A.; Abdullaeva, Z.Sh.; Khudoyberganov, O.I. Synthesis and properties of the coordination compounds calcium stearate with thiocarbamide. *Azerb. Chem. J.* **2023**, 2, 111-115.
23. Sharipova, L.; Ibragimova, M.; Khudoyberganov, O.; Khallokov, F.; Bobakulov, K.; Abdullaeva, Z. Synthesis and study of the complex compound of isonicotinamide with zinc nitrate. *Eurasia Proc. Sci. Technol. Eng. Math.* **2024**, 30, 47-55.
24. Hasanov, Sh.B.; Masharipov, Sh.O.; Ashirov, M.A.; Khudoyberganov, O.I.; Matchanov, A.D.; Abdullaeva, Z.Sh.; Gandjaeva, L.A.; Salimova, S.K.; Babadjanova, S.X. Analysis of the chemical composition of the Cistanche salsa plant growing in the climatic and soil conditions of Khorezm. *Biochem. Cell Arch.* **2024**, 24, 2731-2739.
25. Goldstein, J.I.; Newbury, D.E.; Michael, J.R.; Ritchie, N.W.M.; Scott, J.H.J.; Joy, D.C. *Scanning Electron Microscopy and X-Ray Microanalysis*, 4th ed.; Springer: New York, **2018**; p 201-207.
26. El-Habeeb, A.A.; Refat, M.S. Synthesis, spectroscopic characterizations and biological studies on gold(III), ruthenium(III) and iridium(III) complexes of trimethoprim antibiotic drug. *Bull. Chem. Soc. Ethiop.* **2024**, 38, 701-714.
27. Miessler, G.L.; Fischer, P.J.; Tarr, D.A. *Inorganic Chemistry*, 5th ed.; Pearson: Boston, **2014**; p 341-388.
28. Jingdong, F.; Yingze, S.; Wang, X.Y.; Ye, S.; Yu, Y.H.; Liu, J.X. N-Ligands mediated Co(II) coordination polymer incorporating 5-hydroxyisophthalic acid: Syntheses, structures, and theoretical calculations. *Bull. Chem. Soc. Ethiop.* **2024**, 38, 877-887.
29. Nakamoto, K. *Infrared and Raman Spectra of Inorganic and Coordination Compounds*, Part B: Applications in Coordination, Organometallic, and Bioinorganic Chemistry, 6th ed.; Wiley: Hoboken, NJ, **2009**; p 64-67, 86-88.
30. Amaal, Y.; Al-Assafe, R.A.; Al-Quaba, R.A.S.; Ahmed, A. Synthesis, characterization, and antibacterial studies of some of first transition series metals and zinc complexes with mixed ligands of trimethoprim-isatin and nitrogen base. *Bull. Chem. Soc. Ethiop.* **2024**, 38, 1013-1025.